

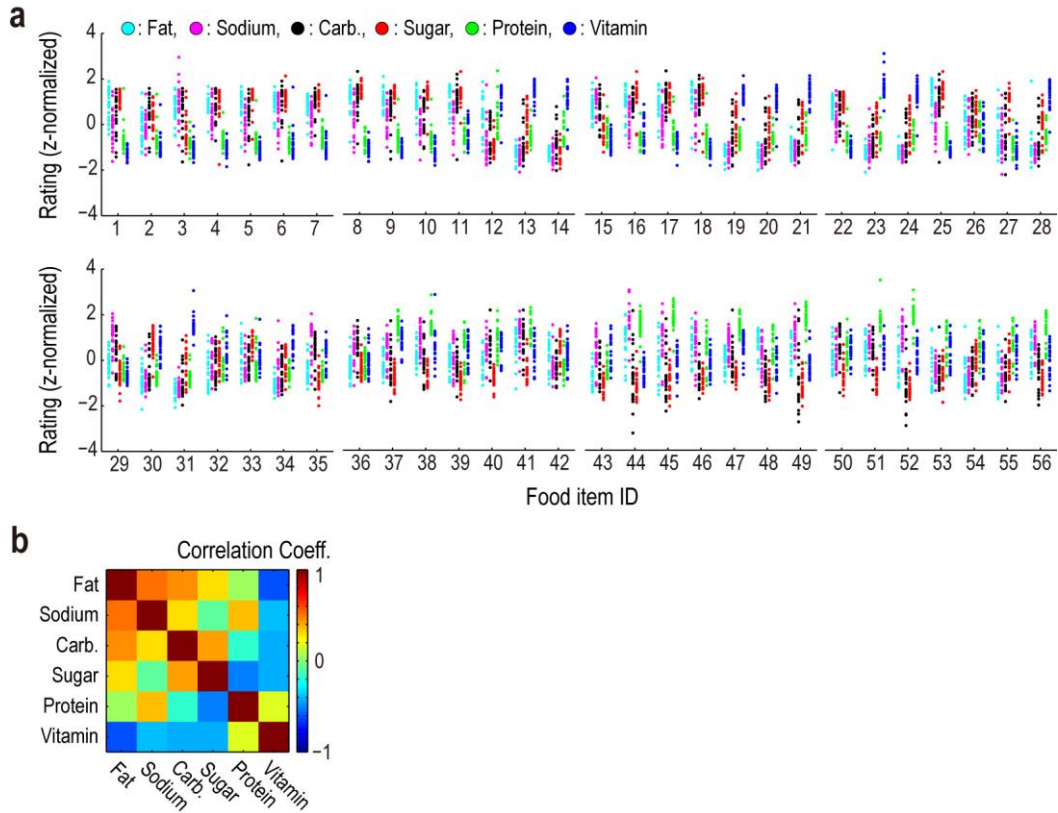
In the format provided by the authors and unedited.

# Elucidating the underlying components of food valuation in the human orbitofrontal cortex

Shinsuke Suzuki <sup>1,2,3\*</sup>, Logan Cross<sup>4</sup> and John P. O'Doherty<sup>1,4</sup>

---

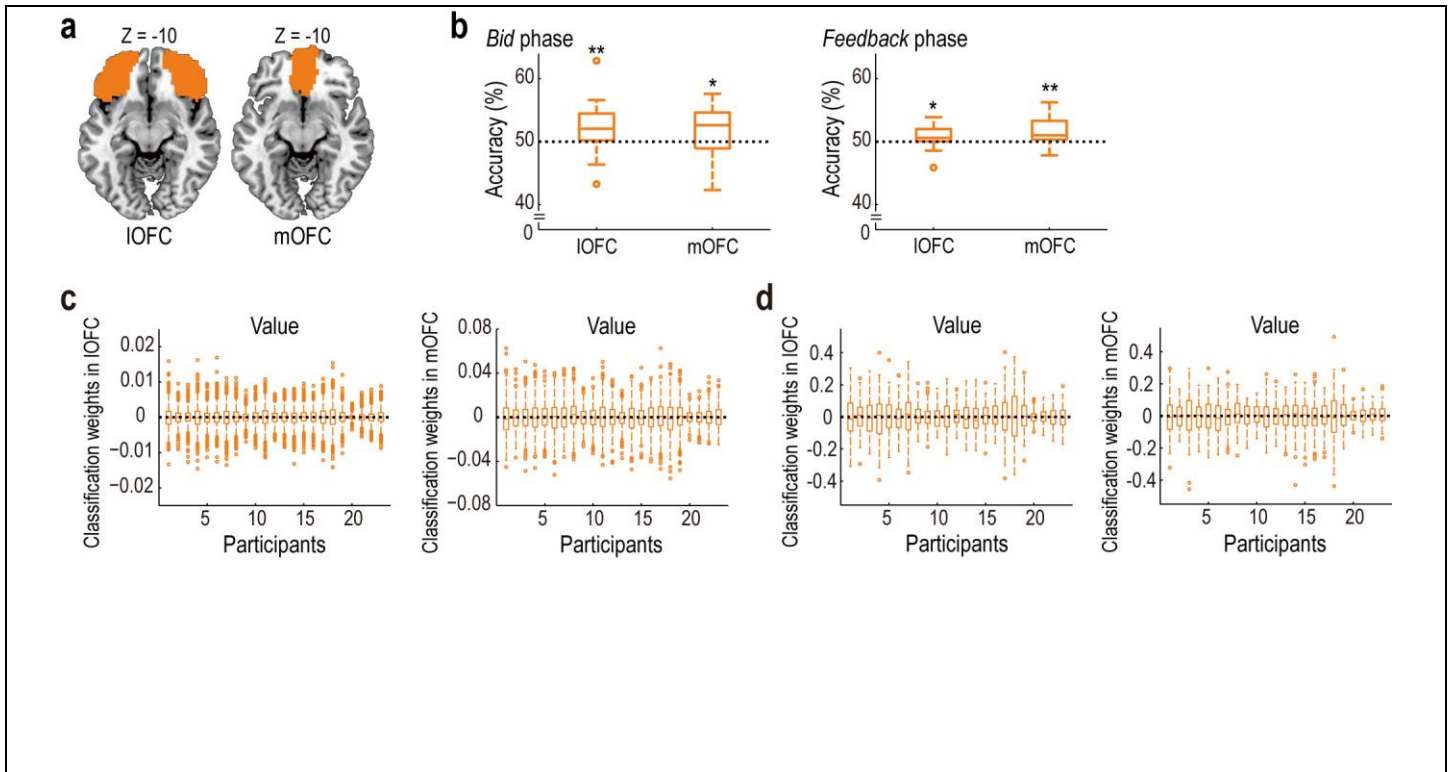
<sup>1</sup>Division of the Humanities and Social Sciences, California Institute of Technology, Pasadena, CA, USA. <sup>2</sup>Frontier Research Institute for Interdisciplinary Sciences, Tohoku University, Sendai, Japan. <sup>3</sup>Institute of Development, Aging and Cancer, Tohoku University, Sendai, Japan. <sup>4</sup>Computation and Neural Systems, California Institute of Technology, Pasadena, CA, USA. \*e-mail: [shinsuke.szk@gmail.com](mailto:shinsuke.szk@gmail.com)



## Supplementary Figure 1

### Ratings of nutrient factors

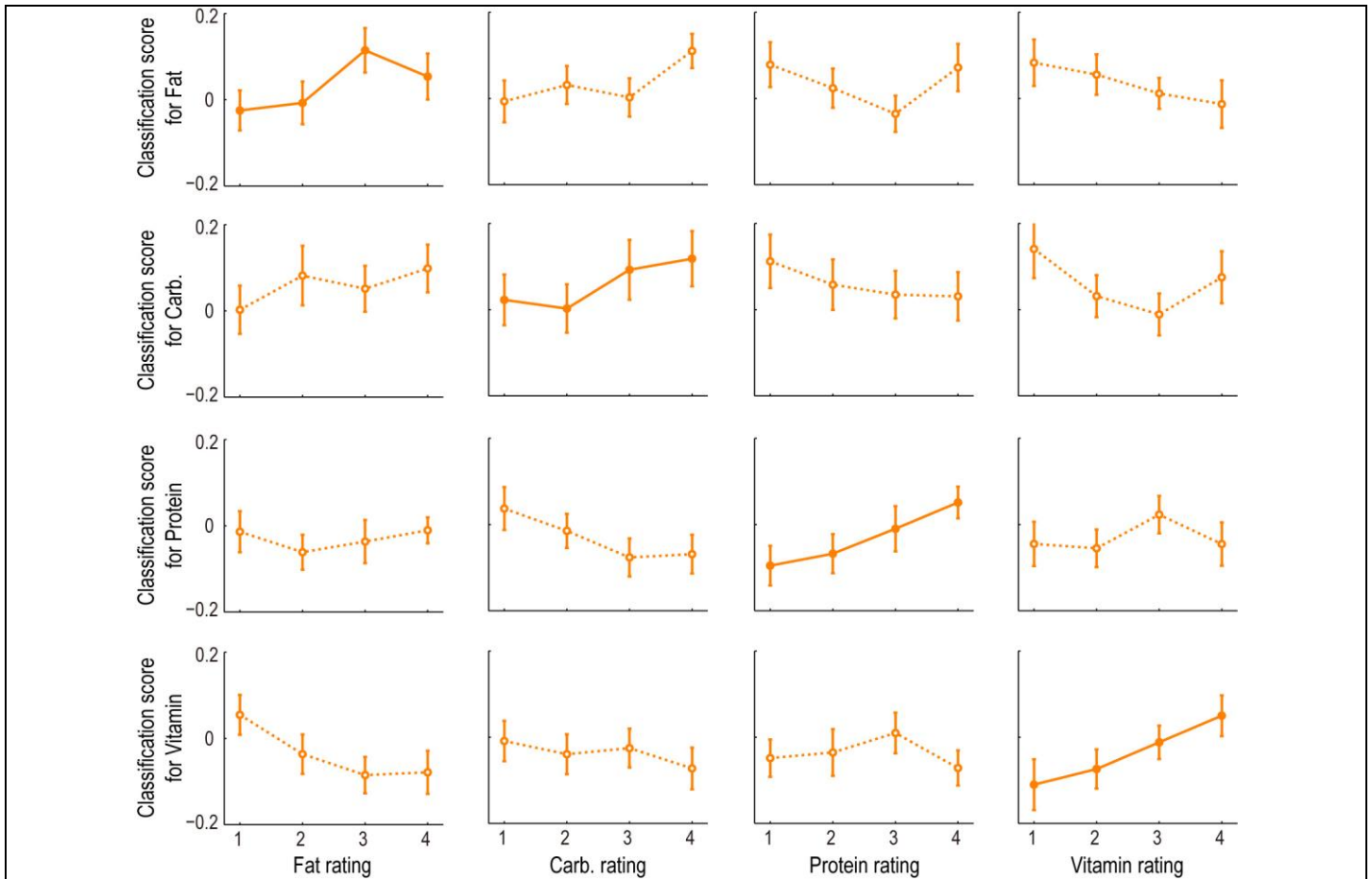
- (a) Subjective ratings about the 56 food items. For each item, we plot the participants' ratings about the six nutrient factors (*cyan*: fat; *magenta*: sodium; *black*: carbohydrate; *red*: sugar; *green*: protein; and *blue*: vitamin). See Table S2 for the item list. The rating data were z-normalized across the food items, within each participant and each nutrient factor.
- (b) Pair-wise correlations among subjective ratings of the nutrient factors (MEAN across participants;  $n = 23$ ).



## Supplementary Figure 2

### Supplementary results of the neural representation of subjective value

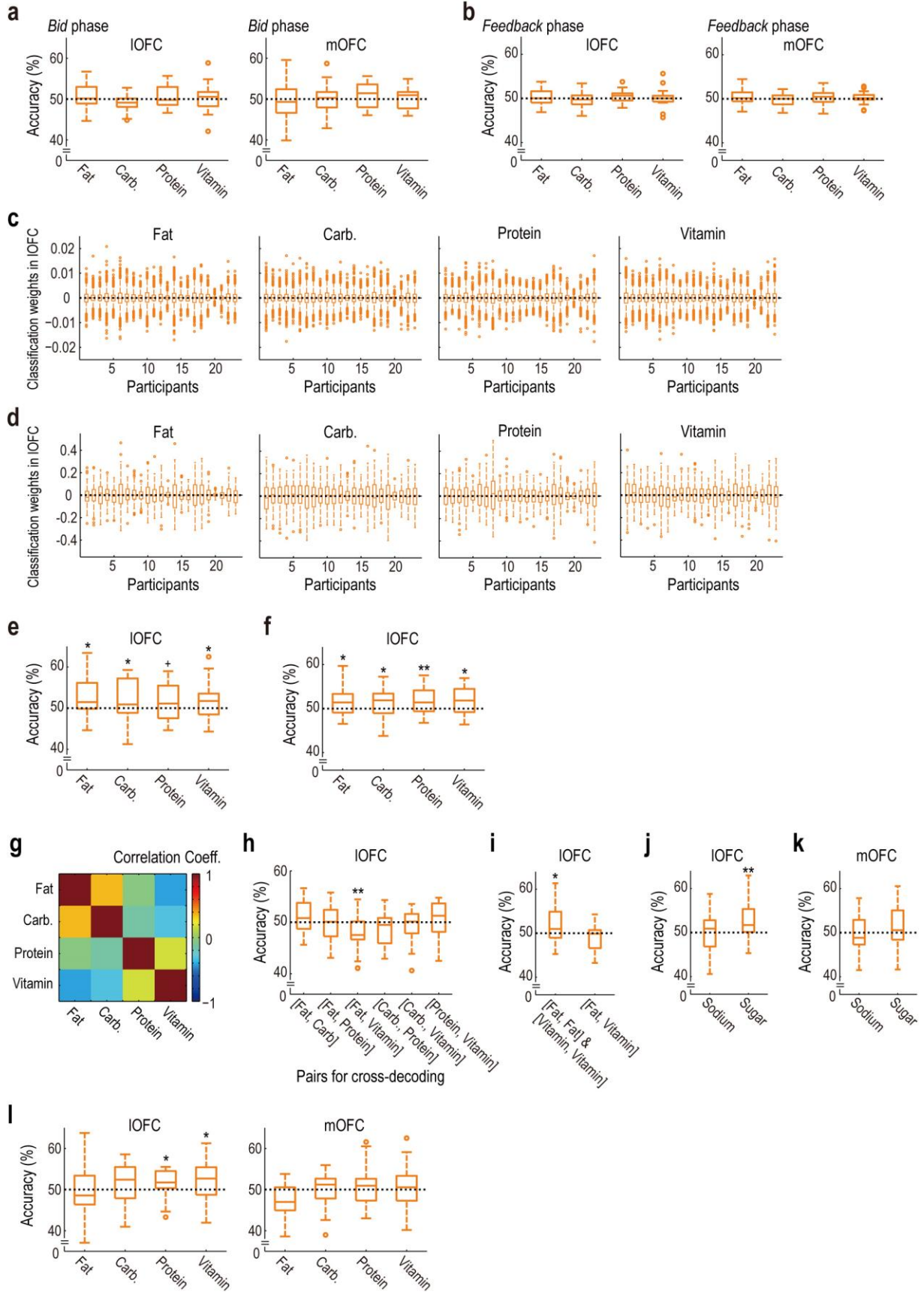
- (a) Anatomical OFC ROIs used in this study. The ROIs are defined based on the AAL database<sup>42</sup> as follows: IOFC, bilateral MNI\_Frontal\_Mid\_Orb + MNI\_Frontal\_Inf\_Orb + MNI\_Frontal\_Sup\_Orb; and mOFC, bilateral MNI\_Frontal\_Med\_Orb. IOFC, lateral orbitofrontal cortex; and mOFC, medial orbitofrontal cortex.
- (b) Evidence for significant decoding of subjective value at the Bid phase (*left*) and at the Feedback phase (*right*) ( $n = 23$  participants). The format is the same as in Fig. 2a (*left*).  $**P < 0.01$  and  $*P < 0.05$ ,  $t$ -test against 50% (Bid phase, IOFC:  $t_{22} = 2.78$ ,  $P = 0.005$ ; mOFC:  $t_{22} = 1.96$ ,  $P = 0.031$ ; and Feedback phase, IOFC:  $t_{22} = 2.23$ ,  $P = 0.018$ ; mOFC:  $t_{22} = 3.40$ ,  $P = 0.001$ ).
- (c) Weights of voxels in the value classifiers obtained from the ROI analyses (see Fig. 2a). We plot the weights of the voxels for each participant within the IOFC (*left*) and the mOFC (*right*) ROIs separately. Format of the box and whisker plots is the same as in Fig. 1c.
- (d) Weights of voxels in the value classifiers obtained from the searchlight analyses (see Fig. 2b). We plot the weights of the voxels within a radius of 3 voxels (i.e., 9mm) around the peak voxels in IOFC (*left*) and mOFC (*right*). See Fig. 2b for information about the peak voxels. Format of the box and whisker plots is the same as in Fig. 1c.



**Supplementary Figure 3**

**Classification scores in the decoding analysis for subjective nutrient factors**

We plot the classification scores in the IOFC ROI obtained by the classifier trained on fat, carb., protein and vitamin respectively as functions of the subjective nutritive ratings (MEAN  $\pm$  SEM across participants;  $n = 23$ ; see Fig. 3a). Note that ratings for each nutrient factors were binned based on the rank order; that each classifier is trained to discriminate high vs. low ratings (i.e., 1 & 2 vs. 3 & 4); and that the classification weights of each voxel were estimated on a subset of the data and the classification scores were computed on the other subset of the data (i.e., leave-one-run-out cross-validation; see Methods for details). IOFC, lateral orbitofrontal cortex; and Carb., carbohydrate.

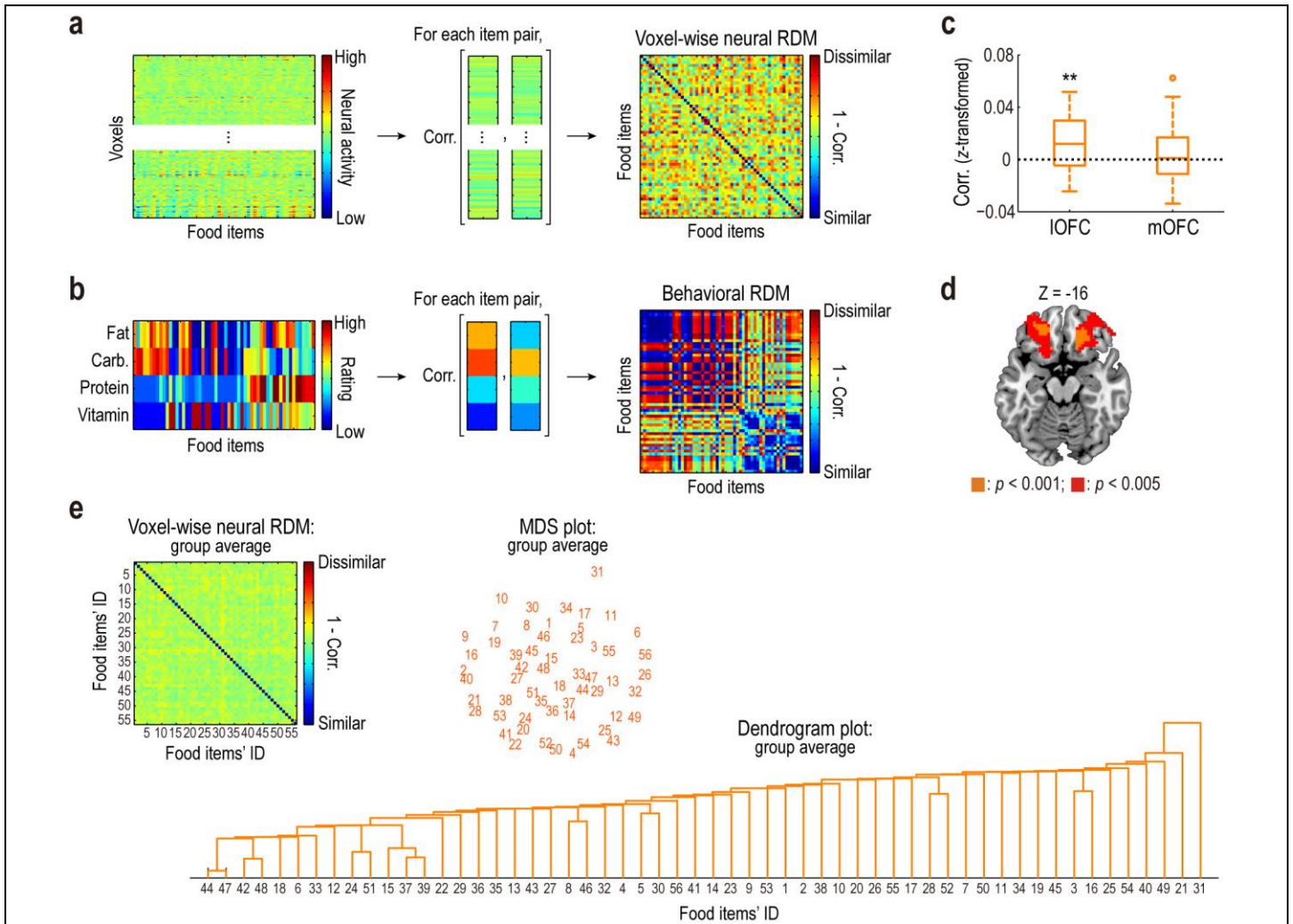


## Supplementary Figure 4

### Supplementary results of the neural representation of subjective nutrient factors

- (a) Decoding accuracies of subjective nutrient factors at the time of bidding revealing a lack of significant decoding at this time-point ( $n = 23$  participants). The format is the same as in Fig. 3a (*left*). *Left*.  $t$ -test against 50% (fat:  $t_{22} = 1.38$ ,  $P = 0.091$ ; carb.:  $t_{22} = -2.47$ ,  $P = 0.989$ ; protein:  $t_{22} = 1.11$ ,  $P = 0.139$ ; and vitamin:  $t_{22} = 0.48$ ,  $P = 0.320$ ). *Right*.  $t$ -test (fat:  $t_{22} = -0.42$ ,  $P = 0.660$ ; carb.:  $t_{22} = 0.14$ ,  $P = 0.444$ ; protein:  $t_{22} = 1.26$ ,  $P = 0.110$ ; and vitamin:  $t_{22} = 0.42$ ,  $P = 0.339$ ). IOFC, lateral orbitofrontal cortex; mOFC, medial orbitofrontal cortex; and Carb., carbohydrate.
- (b) Decoding accuracies of subjective nutrient factors at the time of feedback revealing little evidence for significant decoding at this time-point ( $n = 23$  participants). The format is the same as in Fig. 3a (*left*). *Left*.  $t$ -test against 50% (fat:  $t_{22} = 0.72$ ,  $P = 0.239$ ; carb.:  $t_{22} = -0.43$ ,  $P = 0.664$ ; protein:  $t_{22} = 1.38$ ,  $P = 0.090$ ; and vitamin:  $t_{22} = 0.18$ ,  $P = 0.431$ ). *Right*.  $t$ -test (fat:  $t_{22} = 0.90$ ,  $P = 0.190$ ; carb.:  $t_{22} = -0.80$ ,  $P = 0.783$ ; protein:  $t_{22} = 1.07$ ,  $P = 0.149$ ; and vitamin:  $t_{22} = 1.01$ ,  $P = 0.162$ ).
- (c) Weights of voxels in the classifiers for each of the subjective nutrient factors obtained from the ROI analyses (see Fig. 3a). We plot the weights of the voxels for each participant within the IOFC ROI. Format of the box and whisker plots is the same as in Fig. 1c.
- (d) Weights of voxels in the classifiers for each of the subjective nutrient factors obtained from the search analyses (see Fig. 3a). We plot the weights of the voxels within a radius of 3 voxels (i.e., 9mm) around the peak voxels in IOFC. See Fig. 3c for information about the peak voxels. Format of the box and whisker plots is the same as in Fig. 1c.
- (e) Decoding accuracies of the subjective nutrient factors for novel food items ( $n = 23$  participants). The format is the same as in Fig. 3a (*left*).  $^*P < 0.10$ ,  $^*P < 0.05$  and  $^{**}P < 0.01$  for each factor,  $t$ -test against 50% (fat:  $t_{22} = 2.42$ ,  $P = 0.012$ ; carb.:  $t_{22} = 1.90$ ,  $P = 0.035$ ; protein:  $t_{22} = 1.41$ ,  $P = 0.087$ ; and vitamin:  $t_{22} = 1.84$ ,  $P = 0.039$ ).
- (f) Decoding accuracies of the subjective nutrient factors in the reduced IOFC ROIs ( $n = 23$  participants). In this analysis, (i) we randomly re-sampled adjacent 533 voxels from the IOFC ROI (i.e., forming a continuous cluster consisting of the 533 voxels); then (ii) we tested if information about the subjective nutrient factors could be decoded from the re-sampled voxels; and (iii) the above procedure was repeated 100 times (the decoding accuracies were averaged). The format is the same as in Fig. 3a (*left*).  $^*P < 0.05$  and  $^{**}P < 0.01$  for each factor,  $t$ -test against 50% (fat:  $t_{22} = 2.45$ ,  $P = 0.011$ ; carb.:  $t_{22} = 1.81$ ,  $P = 0.042$ ; protein:  $t_{22} = 2.59$ ,  $P = 0.008$ ; and vitamin:  $t_{22} = 2.46$ ,  $P = 0.011$ ).
- (g) Pair-wise correlations among the classifiers' weights for the four nutrient factors (MEAN across participants;  $n = 23$ ). For each pair of the nutrient factors, we obtained the correlation coefficient in the classification weights of the voxels within the IOFC ROI.
- (h) Decoding accuracies in the cross-decoding analyses ( $n = 23$  participants). Format of the box and whisker plots is the same as in Fig. 1c. Two nutrient factors in each parenthesis denote the pair used for the cross-decoding.  $^{**}P < 0.01$ , two-tailed  $t$ -test against 50% ([fat, carb.]:  $t_{22} = 1.59$ ,  $P = 0.127$ ; [fat, protein]:  $t_{22} = -0.35$ ,  $P = 0.729$ ; [fat, vitamin]:  $t_{22} = -3.18$ ,  $P = 0.004$ ; [carb., protein]:  $t_{22} = -1.96$ ,  $P = 0.062$ ; [carb., vitamin]:  $t_{22} = -1.06$ ,  $P = 0.299$ ; and [protein, vitamin]:  $t_{22} = 0.84$ ,  $P = 0.408$ ).
- (i) Decoding accuracies on the re-sampled food items (see the main text;  $n = 23$  participants). Format of the box and whisker plots is the same as in Fig. 1c. *Left*, accuracy of fat and vitamin (one classifier was trained and tested on fat; the other classifier was on vitamin; and the accuracy scores were averaged). *Right*, accuracy in the cross-decoding analysis between fat and vitamin. Two nutrient factors in the parenthesis denote the pair used for the cross-decoding. That is, we trained a classifier on one factor and tested it on the other factor (and the reverse; and the decoding accuracy was assessed by the average across both directions).  $^*P < 0.05$ , two-tailed  $t$ -test against 50% ([fat, fat] & [vitamin, vitamin]:  $t_{22} = 2.10$ ,  $P = 0.048$ ; and [fat, vitamin]:  $t_{22} = -1.10$ ,  $P = 0.282$ ).
- (j) Significant decoding of sugar but not sodium content in IOFC ( $n = 23$  participants). The accuracies are plotted for the IOFC ROI. Format of the box and whisker plots is the same as in Fig. 1c.  $^{**}P < 0.01$ ,  $t$ -test (Sodium:  $t_{22} = 0.06$ ,  $P = 0.474$ ; and Sugar:  $t_{22} = 2.67$ ,  $P = 0.007$ ).
- (k) Neither sodium nor sugar content was significantly decodable in mOFC ( $n = 23$  participants).  $t$ -test against 50% (Sodium:  $t_{22} = -0.15$ ,  $P = 0.557$ ; and Sugar:  $t_{22} = 1.34$ ,  $P = 0.100$ ). mOFC, medial orbitofrontal cortex. Format of the box and whisker plots is the same as in Fig. 1c.
- (l) Decoding accuracies of objective nutrient factors at the time of valuation, demonstrating relatively weak effects of objective nutrient factors ( $n = 23$  participants). The format is the same as in Fig. 3a (*left*). *Left*.  $^*P < 0.05$ ,  $t$ -test against 50% (fat:  $t_{22} = -0.33$ ,  $P = 0.626$ ; carb.:  $t_{22} = 1.58$ ,  $P = 0.064$ ; protein:  $t_{22} = 2.05$ ,  $P = 0.026$ ; and vitamin:  $t_{22} = 2.26$ ,  $P = 0.017$ ). *Right*.  $t$ -test (fat:  $t_{22} = -3.10$ ,  $P = 0.997$ ; carb.:  $t_{22} = 0.29$ ,  $P = 0.387$ ; protein:  $t_{22} = 0.78$ ,  $P = 0.222$ ; and vitamin:  $t_{22} = 0.08$ ,  $P = 0.469$ ).

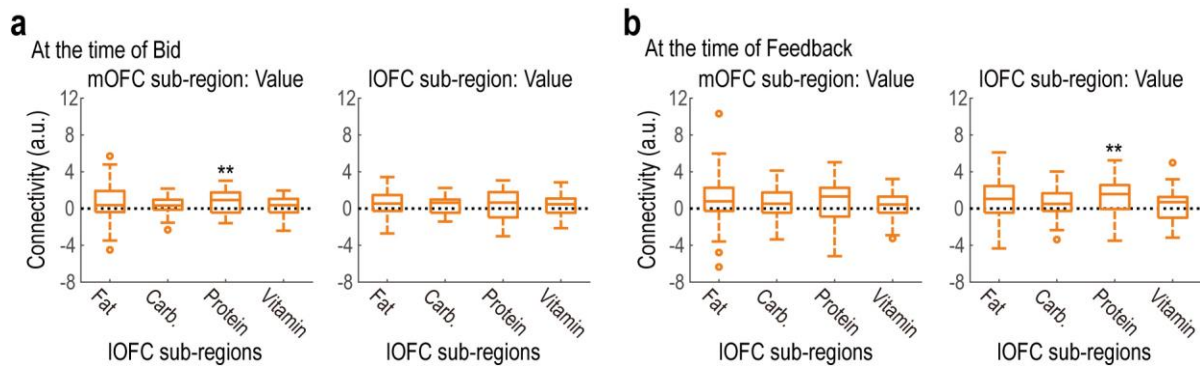




**Supplementary Figure 5**

**Procedure and results of the representational similarity analysis (RSA)**

- (a) Procedure for construction of the voxel-wise Representational Dissimilarity Matrix (RDM). The voxel-wise RDM is created based on the correlation across the voxels' activities for each pair of the items. See Methods for details. Corr., Pearson's correlation coefficient.
- (b) Procedure for construction of the behavioral RDM. The behavioral RDM is created based on the correlation in bundles of the four subjective nutrient factors for each item pair. See Methods for details.
- (c) Results of the ROI analyses. Spearman's rank correlation (z-transformed) between the voxel-wise neural and the behavioral RDMs is plotted for the IOFC and the mOFC ROIs ( $n = 23$ ). Format of the box and whisker plots is the same as in Fig. 1c.  $**P < 0.01$ ,  $t$ -test (IOFC:  $t_{22} = 2.85$ ,  $P = 0.005$ ; and mOFC:  $t_{22} = 1.13$ ,  $P = 0.135$ ). IOFC, lateral orbitofrontal cortex; and mOFC, medial orbitofrontal cortex.
- (d) Results of the searchlight analysis. The RSA correlation map is thresholded at  $P < 0.005$  (uncorrected) for display purposes, generated by performing a  $t$ -test ( $n = 23$  participants). Peak voxels, [MNI:  $x, y, z = 12, 23, -23$ ] and  $[-21, 38, -23]$  ( $P < 0.05$  small-volume corrected) for right and left OFC respectively. OFC, orbitofrontal cortex.
- (e) Pattern of fMRI response to each of the 56 food items in a space of the pair-wise correlation across voxels' activities in the IOFC. We plot the voxel-wise neural RDM averaged over the participants (*top left*,  $n = 23$ ). To visualize the approximate geometric structure, we also show the same data as a two-dimensional MDS plot (*top center*) and a dendrogram plot obtained by an agglomerative hierarchical clustering (*bottom right*). In the MDS plot, the digits depict the food items' ID. See Table S2 for detailed information about the food items. MDS, multi dimensional scaling.

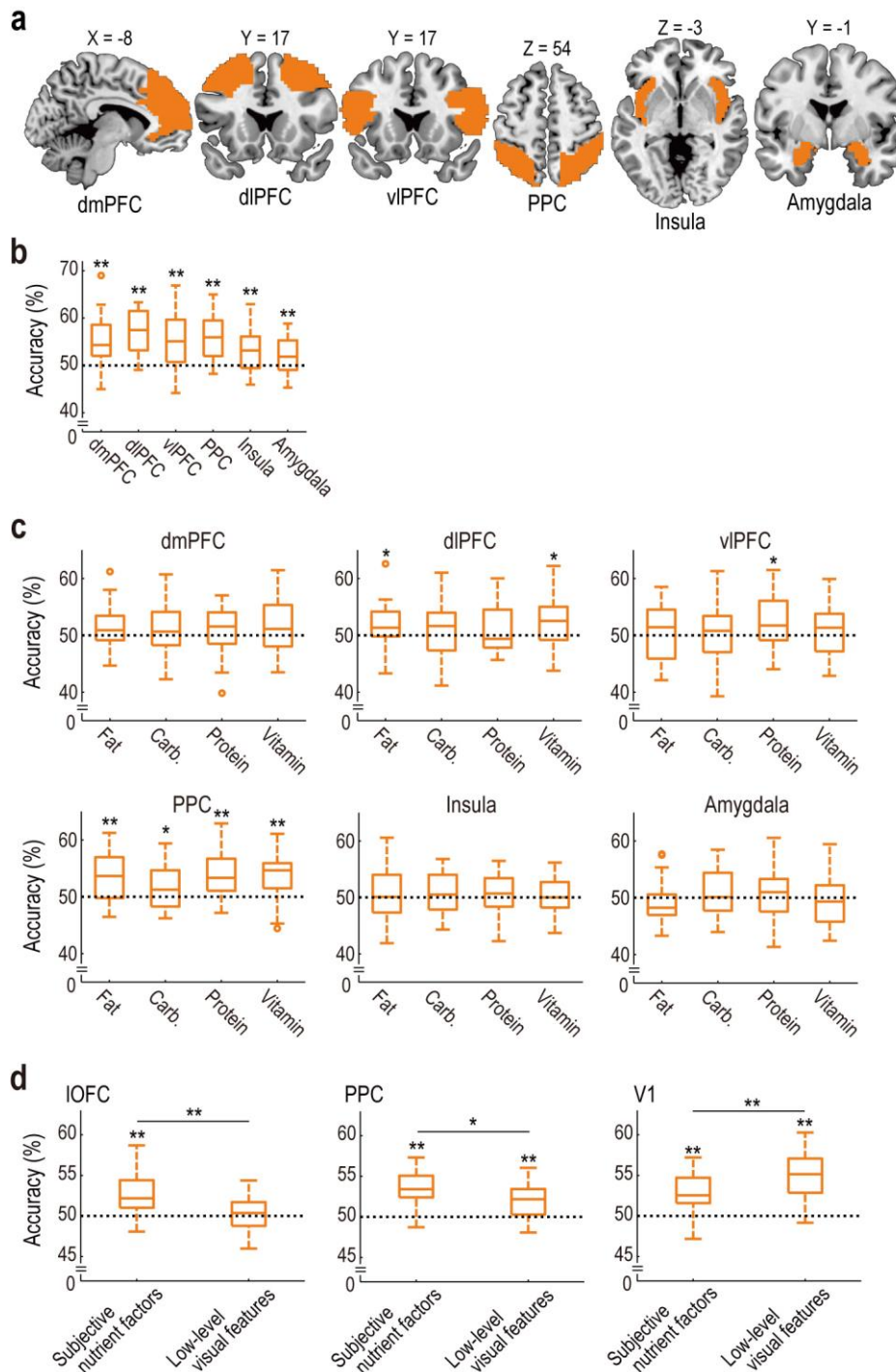


### Supplementary Figure 6

#### Effective connectivity between OFC subregions at the time of bidding and the time of feedback

- (a) Results of an effective connectivity analysis at the time of bidding. Effect sizes of the PPI regressors are plotted ( $n = 23$  participants). The format is the same as in Fig. 5ab. **\*\*** $P < 0.01$  for each factor. *Left.*  $t$ -test (fat:  $t_{22} = 1.37$ ,  $P = 0.092$ ; carb.:  $t_{22} = 1.28$ ,  $P = 0.108$ ; protein:  $t_{22} = 3.20$ ,  $P = 0.002$ ; and vitamin:  $t_{22} = 1.40$ ,  $P = 0.088$ ). *Right.*  $t$ -test (fat:  $t_{22} = 1.59$ ,  $P = 0.063$ ; carb.:  $t_{22} = 1.61$ ,  $P = 0.060$ ; protein:  $t_{22} = 1.54$ ,  $P = 0.068$ ; and vitamin:  $t_{22} = 1.33$ ,  $P = 0.099$ ). IOFC, lateral orbitofrontal cortex; mOFC, medial orbitofrontal cortex; Carb., carbohydrate; and PPI, psychophysiological interaction.
- (b) Results of an effective connectivity analysis at the time of feedback. Effect sizes of the PPI regressors are plotted ( $n = 23$  participants). The format is the same as in Fig. 5ab. **\*\*** $P < 0.01$  for each factor. *Left.*  $t$ -test (fat:  $t_{22} = 1.30$ ,  $P = 0.104$ ; carb.:  $t_{22} = 1.67$ ,  $P = 0.055$ ; protein:  $t_{22} = 1.22$ ,  $P = 0.118$ ; and vitamin:  $t_{22} = 1.02$ ,  $P = 0.159$ ). *Right.*  $t$ -test (fat:  $t_{22} = 1.64$ ,  $P = 0.058$ ; carb.:  $t_{22} = 1.32$ ,  $P = 0.100$ ; protein:  $t_{22} = 2.80$ ,  $P = 0.005$ ; and vitamin:  $t_{22} = 1.01$ ,  $P = 0.161$ ).





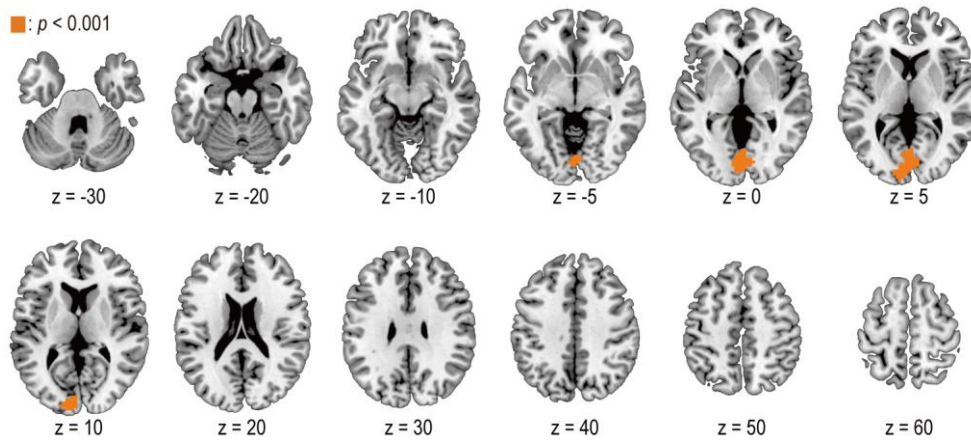
**Supplementary Figure 7**

**Decoding of subjective value and nutrient factors in other brain regions**

(a) Anatomical ROIs used in the additional *post hoc* analyses. The ROIs are defined based on the AAL database<sup>42</sup> as follows: dmPFC, bilateral MNI\_Frontal\_Sup\_Medial + MNI\_Cingulum\_Ant; dlPFC, bilateral MNI\_Frontal\_Mid + MNI\_Frontal\_Sup; vlPFC, bilateral MNI\_Frontal\_Inf\_Oper + MNI\_Frontal\_Inf\_Tri; PPC, bilateral MNI\_Parietal\_Inf + MNI\_Parietal\_Sup; Insula, bilateral MNI\_Insula; and Amygdala, bilateral MNI\_Amygdala. dmPFC, dorsomedial prefrontal cortex; dlPFC, dorsolateral prefrontal cortex; vlPFC,

ventrolateral prefrontal cortex; and PPC, posterior parietal cortex.

- (b) Decoding accuracies of subjective value across the ROIs ( $n = 23$  participants). The format is the same as in Fig. 2a (*left*). \*\* $P < 0.01$  for each region,  $t$ -test against 50% (dmPFC:  $t_{22} = 4.55$ ,  $P < 0.001$ ; dlPFC:  $t_{22} = 7.30$ ,  $P < 0.001$ ; vlPFC:  $t_{22} = 4.39$ ,  $P < 0.001$ ; PPC:  $t_{22} = 6.52$ ,  $P < 0.001$ ; Insula:  $t_{22} = 3.48$ ,  $P = 0.001$ ; and Amygdala:  $t_{22} = 2.92$ ,  $P = 0.004$ ).
- (c) Decoding accuracies of subjective nutrient factors ( $n = 23$  participants). The format is the same as in Fig. 3a (*left*). \* $P < 0.05$  and \*\* $P < 0.01$  for each factor. *Top left*.  $t$ -test against 50% (fat:  $t_{22} = 1.57$ ,  $P = 0.066$ ; carb.:  $t_{22} = 1.12$ ,  $P = 0.137$ ; protein:  $t_{22} = 0.98$ ,  $P = 0.168$ ; and vitamin:  $t_{22} = 1.71$ ,  $P = 0.050$ ). *Top middle*.  $t$ -test (fat:  $t_{22} = 2.25$ ,  $P = 0.018$ ; carb.:  $t_{22} = 1.26$ ,  $P = 0.111$ ; protein:  $t_{22} = 1.52$ ,  $P = 0.071$ ; and vitamin:  $t_{22} = 2.57$ ,  $P = 0.009$ ). *Top right*.  $t$ -test (fat:  $t_{22} = 0.51$ ,  $P = 0.307$ ; carb.:  $t_{22} = 0.52$ ,  $P = 0.305$ ; protein:  $t_{22} = 2.44$ ,  $P = 0.012$ ; and vitamin:  $t_{22} = 0.90$ ,  $P = 0.189$ ). *Bottom left*.  $t$ -test (fat:  $t_{22} = 4.11$ ,  $P < 0.001$ ; carb.:  $t_{22} = 2.37$ ,  $P = 0.014$ ; protein:  $t_{22} = 4.46$ ,  $P < 0.001$ ; and vitamin:  $t_{22} = 4.50$ ,  $P < 0.001$ ). *Bottom middle*.  $t$ -test (fat:  $t_{22} = 0.65$ ,  $P = 0.261$ ; carb.:  $t_{22} = 0.83$ ,  $P = 0.209$ ; protein:  $t_{22} = 0.83$ ,  $P = 0.208$ ; and vitamin:  $t_{22} = 0.05$ ,  $P = 0.481$ ). *Bottom right*.  $t$ -test (fat:  $t_{22} = -0.79$ ,  $P = 0.780$ ; carb.:  $t_{22} = 0.73$ ,  $P = 0.236$ ; protein:  $t_{22} = 0.50$ ,  $P = 0.312$ ; and vitamin:  $t_{22} = -0.23$ ,  $P = 0.592$ ).
- (d) Decoding accuracies of low-level visual features and comparison with subjective nutrient factors in IOFC, PPC and V1. The decoding accuracies of the low-level visual features (averaged over the eight features) and the subjective nutrient factors (averaged over the four factors identified as value predictors) are plotted for the IOFC, the PPC and the V1 (BA17) anatomical ROIs ( $n = 23$  participants). Format of the box and whisker plots is the same as in Fig. 1c. \* and \*\* on each plot respectively denote  $P < 0.05$  and  $P < 0.01$  for each factor,  $t$ -test against 50%. \* and \*\* on the horizontal lines denote significant differences between the indicated pairs of data at  $P < 0.05$  and  $P < 0.01$  respectively, two-tailed paired  $t$ -test. *Left*.  $t$ -test (subjective nutrient factors:  $t_{22} = 4.72$ ,  $P < 0.001$ ; low-level visual features:  $t_{22} = 0.70$ ,  $P = 0.247$ ; and subjective nutrient factors vs. low-level visual features:  $t_{22} = 3.18$ ,  $P = 0.004$ ). *Middle*.  $t$ -test (subjective nutrient factors:  $t_{22} = 7.04$ ,  $P < 0.001$ ; low-level visual features:  $t_{22} = 4.01$ ,  $P < 0.001$ ; and subjective nutrient factors vs. low-level visual features:  $t_{22} = 2.62$ ,  $P = 0.0157$ ). *Right*.  $t$ -test (subjective nutrient factors:  $t_{22} = 5.85$ ,  $P < 0.001$ ; low-level visual features:  $t_{22} = 8.34$ ,  $P < 0.001$ ; and subjective nutrient factors vs. low-level visual features:  $t_{22} = 3.15$ ,  $P = 0.005$ ). IOFC, lateral orbitofrontal cortex; PPC, posterior parietal cortex; V1, primary visual cortex; and BA17, Brodmann area 17.



### Supplementary Figure 8

#### A region of V1 in which all of the four subjective nutrient factors can be decoded

The decoding accuracy map obtained from the whole-brain searchlight analysis is thresholded at  $P < 0.05$  (cluster-level FWE correction with the cluster-forming threshold  $P = 0.001$ ;  $n = 23$  participants), conjunction-test. Peak voxel, [MNI: x, y, z = -9, -94, 7]. V1, primary visual cortex.

**Table S1. Prediction performances of the subjective value.**

	Rank	Explanatory variables	Performance
<i>Linear regression</i>	<b>1</b>	<b>fat, carbohydrate, protein, vitamin</b>	<b>0.481</b>
	2	fat, sodium, carbohydrate, protein, vitamin	0.478
	3	fat, sodium, protein, vitamin	0.474
	4	fat, protein, vitamin	0.465
	5	sodium, carbohydrate, protein, vitamin	0.463
	6	fat, sodium, sugar, protein, vitamin	0.455
	7	fat, carbohydrate, sugar, protein, vitamin	0.455
	8	carbohydrate, protein, vitamin	0.453
	9	fat, sodium, carbohydrate, sugar, protein, vitamin	0.452
	10	fat, sugar, protein, vitamin	0.440
<i>Logistic regression</i>	<b>1</b>	<b>fat, carbohydrate, protein, vitamin</b>	<b>69.95%</b>
	2	fat, sodium, carbohydrate, protein, vitamin	69.64%
	3	sodium, carbohydrate, protein, vitamin	69.26%
	4	fat, protein, vitamin	69.10%
	5	fat, sodium, protein, vitamin	68.94%
	6	fat, sodium, carbohydrate, protein	68.79%
	7	sodium, protein, vitamin	68.79%
	8	carbohydrate, protein, vitamin	68.79%
	9	fat, sodium, carbohydrate, sugar, protein	68.48%
	10	sodium, carbohydrate, sugar, protein, vitamin	68.25%

Prediction performances of the best 10 models are shown for linear and logistic regression analyses (the best model in each analysis is shown in bold). Performance, z-transformed correlation between the predicted and the actual values for the linear regression analysis, and prediction accuracy for the logistic regression analysis. See Methods for details.

**Table S2. Food items used**

---

1. 3 Musketeers <sup>d</sup>	29. Sun Chips <sup>e</sup>
2. Barnum's Animal Crackers <sup>d</sup>	30. Dole Mixed Fruit <sup>a</sup>
3. Doritos Nacho Cheese <sup>e</sup>	31. Grapefruit <sup>a</sup>
4. Chips Ahoy! <sup>d</sup>	32. Banana Chips <sup>e</sup>
5. Kit Kat <sup>d</sup>	33. Dark Chocolate Bananas <sup>d</sup>
6. Pop-Tarts Brown Sugar Cinnamon <sup>d</sup>	34. Crispy Apple <sup>e</sup>
7. Pop-Tarts Frosted Strawberry <sup>d</sup>	35. Vegetable Chips <sup>e</sup>
8. Hostess Powdered Donettes <sup>d</sup>	36. Sweet Potato Chips <sup>e</sup>
9. Twix Cookie Bars <sup>d</sup>	37. Chopped Salad Chicken <sup>c</sup>
10. Hershey's Whatchamacallit Candy <sup>d</sup>	38. Mexicali Salad <sup>c</sup>
11. Apple Pie <sup>d</sup>	39. Caesar Salad <sup>c</sup>
12. Avocado <sup>a</sup>	40. Veggie Wrap <sup>c</sup>
13. Blackberries <sup>a</sup>	41. Super Burrito <sup>c</sup>
14. Cauliflower <sup>a</sup>	42. Chocolate & Berry <sup>d</sup>
15. Ritz Crackers'n Cheese Dip <sup>e</sup>	43. Green Beans Chips <sup>e</sup>
16. Cherry Pie <sup>d</sup>	44. Salami <sup>b</sup>
17. Chocolate Muffins <sup>d</sup>	45. Smoked Turkey <sup>b</sup>
18. Hostess Donettes <sup>d</sup>	46. American Cheese <sup>b</sup>
19. Granny Smith Apple <sup>a</sup>	47. Chicken & Roasted Beet <sup>c</sup>
20. Green Grapes <sup>a</sup>	48. Mozzarella Cheese <sup>b</sup>
21. Mango <sup>a</sup>	49. Roast Beef <sup>b</sup>
22. Milano Cookies <sup>d</sup>	50. Caprese Sandwich <sup>c</sup>
23. Orange <sup>a</sup>	51. Tuna Salad Wrap <sup>c</sup>
24. Raspberries <sup>a</sup>	52. Smoked Salmon <sup>b</sup>
25. Red Velvet Cake <sup>d</sup>	53. Plain Yogurt <sup>b</sup>
26. Quaker Chewy Granola Bar <sup>d</sup>	54. Strawberry Yogurt <sup>b</sup>
27. Starburst Candy <sup>d</sup>	55. Blueberry Yogurt <sup>b</sup>
28. Strawberry <sup>a</sup>	56. Deviled Eggs <sup>b</sup>

---

<sup>a</sup> fresh vegetables and fruits (e.g., Orange and Apple), <sup>b</sup> meet and dairy products (e.g., salami and yogurt), <sup>c</sup> cooked products (e.g., salad and wrap), <sup>d</sup> sweet snacks (e.g., chocolate bar and cake), and <sup>e</sup> salty snacks (e.g., chips and crackers).